

Experimental investigation of an unusual induction effect and its interpretation as a necessary consequence of Weber electrodynamics

Steffen Kühn¹

The magnetic component of the Lorentz force acts exclusively perpendicular to the direction of motion of a test charge, whereas the electric component does not depend on the velocity of the charge. This article provides experimental indication that, in addition to these two forces, there is a third electromagnetic force that (i) is proportional to the velocity of the test charge and (ii) acts parallel to the direction of motion rather than perpendicular. This force cannot be explained by the Maxwell equations and the Lorentz force, since it is mathematically incompatible with this framework. However, this force is compatible with Weber electrodynamics and Ampère’s original force law, as this older form of electrodynamics not only predicts the existence of such a force but also makes it possible to accurately calculate the strength of this force.

Keywords: Weber electrodynamics, Ampère’s force law, non-Lorentzian forces, Lorentz force, Maxwell equations

1 Introduction

As generally accepted, the electromagnetic force \mathbf{F} onto a test charge q with velocity \mathbf{v} is fully given by the two fields \mathbf{E} and \mathbf{B} and the Lorentz force

$$\mathbf{F} = q\mathbf{E} + q\mathbf{v} \times \mathbf{B}. \quad (1)$$

As seen, the formula of the Lorentz force (1) cannot express a force component proportional to $q\mathbf{v}$, because (i) $q\mathbf{E}$ is independent of \mathbf{v} and (ii) the term $\mathbf{v} \times \mathbf{B}$ is always oriented perpendicular to \mathbf{v} . Thus, should there be an electromagnetic force that is proportional to the speed of the test charge and acts parallel to the direction of motion, it would be intrinsically incompatible with the Lorentz force (1).

However, the experiment performed in this article provides indication that such a force exists. Although the existence of this force may seem highly implausible after more than a century of practical experience in electrical engineering, these forces only occur, when comparatively strong displacement currents are present. Moreover, there has been little reason to study or search for unexpected effects in century-old theories.

Despite the low importance of the force in conventional engineering, it is not the first time that such a force has been reported [1]. André-Marie Ampère explicitly investigated this kind of force experimentally and, in 1822, deduced the equation

$$\mathbf{F} = \frac{\mu_0 ds^2}{4\pi r^3} \mathbf{r} \left(3 \frac{(\mathbf{r} \cdot \mathbf{i}_s)(\mathbf{r} \cdot \mathbf{i}_d)}{r^2} - 2 \mathbf{i}_s \cdot \mathbf{i}_d \right), \quad (2)$$

for the force of a current element $ds \mathbf{i}_s$ of length ds at the origin onto another current element $ds \mathbf{i}_d$ at \mathbf{r} [2–5].

This equation can be interpreted by using Weber electro-dynamics, which is older than Maxwell’s electro-dynamics. The core of Weber electro-dynamics is a force formula that resembles Coulomb’s law. But, in contrast to Coulomb’s law, Weber’s formula contains not only the distance between the charges as a parameter but also the relative speed and acceleration of the charges.

Because Weber’s formula is a force law without fields, it is not suitable for explaining electromagnetic waves. This is not a principle-related deficiency, and some attempts have been made to extend Weber electro-dynamics accordingly (eg [6]). However, only a few scientists have known about Weber’s electro-dynamics since the beginning of the 20th century, although a small community still actively researches and works on this topic [7–15]. Therefore, these adjustments failed to gain acceptance and were scarcely noticed by most physicists and engineers. However, even without such extensions, Weber’s law of force is a remarkably simple and powerful approach that can probably explain all quasi-stationary effects [16–18].

The simplest way to understand Weber’s law of force from a modern point of view is to assume that the potential energy between two point charges q_s and q_d at the locations \mathbf{r}_s and \mathbf{r}_d , respectively, is given by the formula

$$V = \frac{1}{\gamma(\dot{r})} V_C(r), \quad (3)$$

where

$$V_C(r) = \frac{q_s q_d}{4\pi \epsilon_0 r}, \quad (4)$$

is the classical potential energy of two point charges at rest with respect to each other [19, 20]. In this formula, $r := \|\mathbf{r}\|$ is the distance between the two point charges; that is, the Euclidean norm of the distance vector

$$\mathbf{r} = \mathbf{r}_d - \mathbf{r}_s. \quad (5)$$

¹ Aurinovo GmbH, Werder, Germany, independent researcher, steffen.kuehn@aurinovo.de

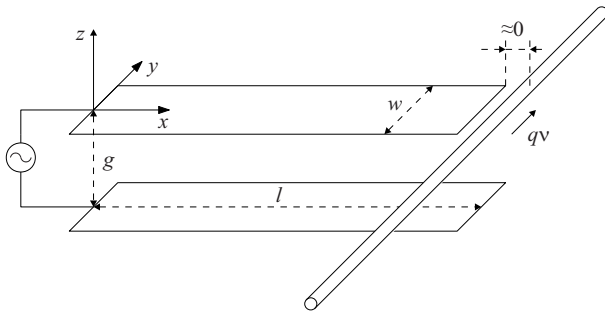


Fig. 1. The principle of the experiment is to determine whether, during the charging and discharging of a capacitor (left), a force is generated on fast-moving charge carriers in a tube (right), and whether this force is proportional to the speed of the charge carriers and acts in their direction of motion.

As per convention, the dot on top of a symbol indicates the derivative with respect to time. Therefore, $\dot{r} = \dot{\mathbf{r}} \cdot \mathbf{r}/r$ is not the differential velocity $\dot{\mathbf{r}} = \dot{\mathbf{r}}_d - \dot{\mathbf{r}}_s$ nor its Euclidean norm. \dot{r} is instead the relative speed, *ie* the speed with which the two charges approach or move away from each other on their connecting line.

$\gamma(v) = 1/\sqrt{1 - v^2/c^2}$ is the Lorentz factor known from special relativity, where c is the speed of light in vacuum. If the relative speed \dot{r} between the two point charges is zero, the Lorentz factor is equal to one, and Equation (3) becomes the usual formula for the potential energy of a resting point charge interacting with another resting point charge (4).

For small relative speeds \dot{r} , which can be verified by calculating the Taylor series, the approximation

$$V \approx \left(1 - \frac{\dot{r}^2}{2c^2}\right) \frac{q_s q_d}{4\pi\epsilon_0 r}, \tag{6}$$

can be obtained. This formula appears for the first time in 1848 in a publication by Wilhelm Weber [18]. The corresponding force formula for the potential energy (6) is

$$\mathbf{F} = \frac{q_s q_d}{4\pi\epsilon_0} \frac{\mathbf{r}}{r^3} \left(1 - \frac{\dot{r}^2}{2c^2} + \frac{r\ddot{r}}{c^2}\right). \tag{7}$$

This force formula dates back to 1846 [18]. The relationship between the Weber force (7) and potential energy (6) can be verified in a few steps and is given by

$$-\dot{V} = \mathbf{F} \cdot \dot{\mathbf{r}}, \tag{8}$$

which is an alternative representation of the law of energy conservation, as the term on the right side represents the time derivative of the kinetic energy.

Equation (7) expresses the force between two electric point charges. However, most macroscopic considerations involve electric currents. An electric current is a multi-particle phenomenon. For example, a current could be a metal wire with positively charged ions at rest and negatively charged electrons moving at a non-zero drift velocity.

A unique feature of Weber’s force law is that the original form of Ampère’s force law can be derived from Weber’s law without additional assumptions [21]. This means that the Weber force is a microscopic explanation of the magnetic forces between arbitrarily shaped conductor loops. This interpretation is noteworthy given the simplicity of the potential energy expression (3), it suggests that one could work without a vector potential, magnetic field, or Lorentz force (1).

It should also be noted that the Weber force satisfies the conservation laws for momentum, angular momentum, and energy in its strong form. The Liénard-Schwarzschild force (equation (8) in reference [18]), which is the counterpart to Weber’s force that follows from Maxwell’s equations, violates these conservation laws [22].

The next section of this article describes an experiment in which an unusual aspect of Weber electrodynamics comes into play. The third section provides a detailed theoretical analysis of this effect.

2 Experiment

2.1 Concept

The basic concept of this experiment is to determine whether fast-moving charge carriers that are moving sideways past the plate of a capacitor perceive a force in their direction of motion when the plate capacitor is charged and discharged by an alternating current. Figure 1 shows the principle of the experiment.

As the sketch in Fig. 1 suggests, the experiment is conducted by placing a long tube with fast-moving electrons near one of the plates of a plate capacitor. The capacitor (left side of Fig. 1) acts as an antenna and produces a slowly oscillating electromagnetic field. The exact shape of the electromagnetic field is not relevant for this experiment because neither the magnetic nor the electric component is able to generate a force or voltage in the tube proportional to the speed of the charge carriers in the tube. This aspect can be seen by substituting the fields \mathbf{E} and \mathbf{B} and the velocity $\mathbf{v} = v\mathbf{e}_y$ into the Lorentz force (1) and multiplying by \mathbf{e}_y , *ie*, by the direction of motion of the charge carriers in the tube. The resulting force component is $q\mathbf{e}_y \mathbf{E}$, which clearly does not depend on the speed v .

It should be mentioned that the current in the tube also generates a magnetic field. As is obvious from the geometry, this magnetostatic field produces a force in the y -direction on the current in the capacitor. In other words, standard electrodynamics predicts that the current in the capacitor has no effect in the y -direction on the current in the tube yet simultaneously claims that the current in the tube produces a force in the y -direction on the current in the capacitor.

For logical reasons, the force postulated in this article should exist, and its apparent existence is not surprising. However, this finding is unfortunately also an indication that standard electrodynamics, or at least the Lorentz

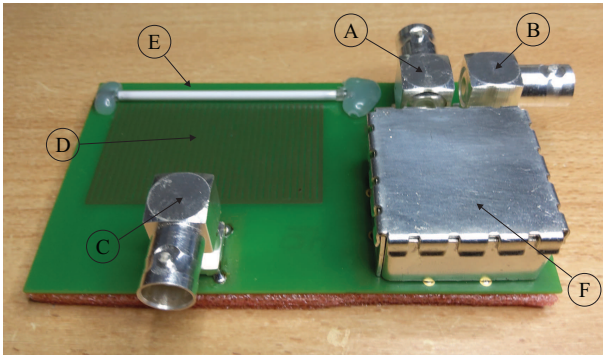


Fig. 2. Circuit board: (a) – connection for a high DC voltage to operate the tube, (b) – measuring connector, (c) – input feed to the transmit antenna, (d) – capacitor as the transmit antenna, (e) – receiver tube, – shielded receiver circuit

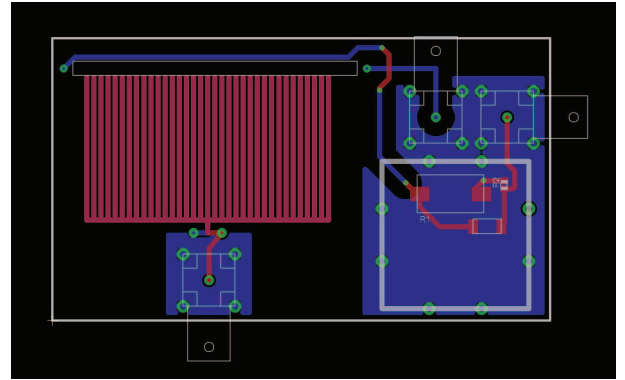


Fig. 3. Printed circuit board with receiver and transmit capacitor. The top side is shown in red, and the bottom side is shown in blue

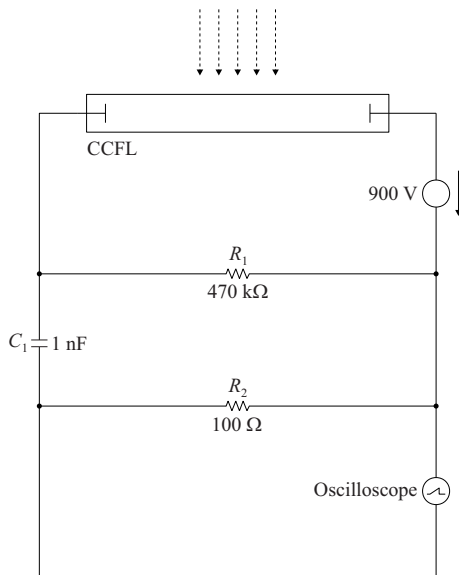


Fig. 4. Circuit of the receiver, shown without the transmit capacitor

force, could be incomplete. In Weber electrodynamics, this strange asymmetry does not exist.

2.2 Implementation

The experiment was performed using a $6.0\text{ cm} \times 10.5\text{ cm}$ double-layer printed circuit board (PCB) that was 1 mm thick and made of FR4. Figure 2 is a photograph of the exact circuit board used in this experiment.

As shown in Fig. 2, there are three BNC connectors on the board. The first BNC connector (A) is for connecting a 900 V DC voltage to operate the tube. Socket (B) is the connection for the oscilloscope, and socket (C) is for connecting a waveform generator to capacitor (D). The capacitor is comb-shaped both on top and bottom of the board and has a capacitance of 37 pF. The reasons for choosing this shape of capacitor will be described in the theory section of this article. The metal case (F) in Fig. 2 contains a few components that are shielded against electromagnetic interference. The ground of the housing

is connected to the ground for sockets (A) and (B), but not with the ground for socket (C).

The receiver (E) is a type BF2661-24B cold-cathode fluorescent lamp (CCFL) from the manufacturer JKL. The tube emits UV radiation at a wavelength of $\lambda = 253.7\text{ nm}$ [23]. A CCFL is a type of tube in which the electrons are only drawn from the cathode by the high intensity of the electric field. Because the tube contains a gas rather than a vacuum, the speed v of the electrons is not proportional to the applied voltage and can therefore only be estimated to be approximately $0.0076 c$ using the following equation:

$$\frac{1}{2} m_e v^2 = h \frac{c}{\lambda}, \quad (9)$$

where m_e is the mass of the electron and h is Planck's constant. This experiment used a CCFL tube because the external dimensions imposed tight constraints and a sufficiently thin tube with a Wehnelt cylinder and without gas filling was not available as a component.

Figure 3 shows the layout of the two-layer PCB, with the top layer shown in red and the bottom layer in blue. The corresponding circuit, without the capacitor (D) serving as the transmit antenna, is shown in Fig. 4. The circuit consists only of a load resistor R1, which limits the current through the tube to 1.39 mA, and a passive high-pass filter. The high-pass filter consists of a high-voltage capacitor C1 and a resistor R2 that decouple the measurement connector (B) from the high voltage and filters out frequencies below $\approx 1\text{ MHz}$.

Components R1, R2, and C1 are located under a shielded metal housing and above a ground plane on the bottom side of the PCB. The traces outside the housing were designed to be as short as possible. The area of the receiving antenna's conductor loop was minimized; however, some compromises had to be made with this design, as the high voltage imposed minimum distances.

2.3 Results

The first measurement of the experiment was performed without the tube soldered in. This was done to

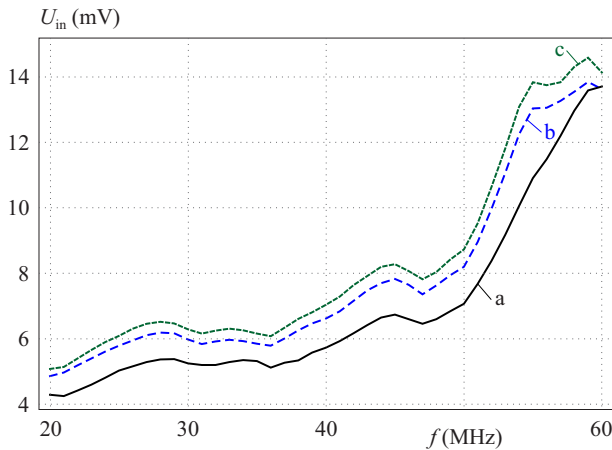


Fig. 5. Measured amplitudes as a function of the transmission frequency: (a) – without tube, (b) – with tube but without high voltage, (c) – with tube and high voltage.

determine how strongly the feed line of the tube would act as an electrical antenna for parasitic longitudinal electric fields. For this purpose, a sinusoidal voltage with an amplitude of 2.5 V and a frequency of 20–60 MHz was applied to the BNC socket (C). The frequency of the signal was increased stepwise by 1 MHz.

A digital oscilloscope (PicoScope 3206D, $\pm 200\text{mV}$, 500MS/s) was used for the measurement. The evaluation was performed in the frequency domain with PicoScope® 6 software (8192 spectrum bins, Gaussian window) and the operator “Average Amplitude at Peak”, which provides the average value and the standard deviation σ in the range of the strongest signal peak, which always clearly had the same frequency as the injected signal.

The result is shown in Fig. 5 as a black solid line (A). In this experiment, it turned out that it made no difference whether the high voltage (U33010/3B Scientific) was on or off, as the measured curve was almost identical in both cases. The amplitude of the measured signal frequency was also two to three orders of magnitude higher than that of interfering frequencies and was therefore clearly distinguishable.

After the tube was installed, the experiment was repeated twice, once with the high voltage source off and once with it on. The results are shown as curves (B) and (C) in Fig. 5, where curve (B) was measured with the high voltage switched off. Even with the tube turned off, the amplitude generally increased by about 1.5 mV compared to curve (A) measured without the tube present. This would be expected, as the gas in the tube can be polarized and therefore reacts to parasitic electric fields in the longitudinal direction of the tube.

The amplitude was further increased when the high voltage was switched on (*ie*, when the electrons in the tube were moving with a drift speed of approximately $0.0076c$). This is remarkable and cannot be explained by the longitudinal electric field component, as the electric force does not depend on the speed of the charge carriers

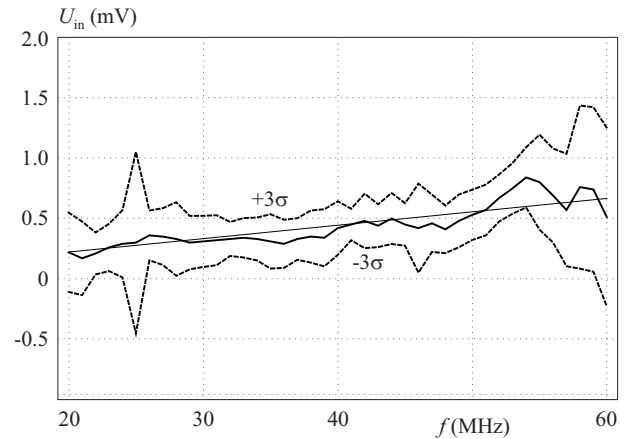


Fig. 6. The measured voltage difference between the experiments run with high voltage switched off and on, with dashed curves indicating the 3σ confidence interval, thin line the linear fit of the measured curve with slope of 11.1 pV/Hz

and a magnetic field cannot accelerate charge carriers in the direction of motion.

If we calculate the difference between the curves (C) and (B), we obtain the curve shown in Fig. 6, which shows a linear frequency dependence. This is consistent with Weber electrostatics, as will become evident in the theory section.

3 Theory

3.1 Current in the transmitter

To analyze the experimental results, we first need to find the current $i(x, t)$ in the transmit capacitor (D) in Fig. 2. As shown in Fig. 1, a single tooth of the comb-shaped capacitor can be schematically interpreted as a biplanar microstrip with a sinusoidal AC voltage $u(t) = u(x = 0, t) = U_0 e^{i\omega t}$, amplitude U_0 , and angular frequency ω applied to its input at $x = 0$.

To calculate the current, we consider the microstrip to be an unterminated transmission line. The telegrapher’s equations can be applied in this context, and it is therefore possible to use Equation (15) from reference [24] to calculate the transfer function. Because the transmission line is unterminated in this example, the termination impedance is $Z_T \rightarrow \infty$. Equation (15) from reference [24] therefore simplifies to

$$H = \frac{\cosh\left((l-x)\sqrt{\frac{Z'_L}{Z'_Q}}\right)}{\cosh\left(l\sqrt{\frac{Z'_L}{Z'_Q}}\right)}. \quad (10)$$

In this equation,

$$Z'_L = i\omega L', \quad (11)$$

is the series impedance, with L' being the inductance per meter, and

$$Z'_Q = \frac{1}{i\omega C'}, \quad (12)$$

where C' is the capacitance per meter. The series resistance is neglected as irrelevant.

Equation (16) from reference [24] defines the voltage

$$u(x, t) = H U_0 e^{i\omega t}, \quad (13)$$

along the microstrip, and Equation (20) gives the current

$$i(x, t) = -\frac{1}{Z'_L} \frac{\partial H}{\partial x} U_0 e^{i\omega t}. \quad (14)$$

Substituting Equation (10) into these expressions gives

$$u(x, t) = \frac{\cos\left(\sqrt{L' C'} \omega (l - x)\right)}{\cos\left(\sqrt{L' C'} \omega l\right)} U_0 e^{i\omega t}, \quad (15)$$

and

$$i(x, t) = \sqrt{\frac{C'}{L'}} \frac{\sin\left(\sqrt{L' C'} \omega (l - x)\right)}{\cos\left(\sqrt{L' C'} \omega l\right)} U_0 e^{i\left(\omega t + \frac{\pi}{2}\right)}. \quad (16)$$

The maximum frequency in the described experiment was 60 MHz, which corresponds to a wavelength of 5 m. Because this is a long wavelength relative to the length $l = 3$ cm of the capacitor, the voltage (15) and current (16) can be approximated using the first order Taylor series with respect to ω . This simplifies (15) and (16) to

$$u(x, t) \approx u(t) = U_0 e^{i\omega t}, \quad (17)$$

and

$$i(x, t) \approx C' \omega (l - x) U_0 e^{i\left(\omega t + \frac{\pi}{2}\right)}. \quad (18)$$

As these equations show, the voltage everywhere in the capacitor is equal to the input voltage. However, as expected, the current precedes the voltage by 90° , decreases linearly and disappears completely by the end of the line. The inductance per meter L' has no effect. Because the experiment uses a simple plate capacitor, the capacitance per meter C' can be defined as

$$C' = \frac{\epsilon_r \epsilon_0 w}{g}, \quad (19)$$

where ϵ_r is the relative permittivity of the medium between the plates. Using the parameters of the capacitor in our experiment ($\epsilon_r = 4$, $w = 1$ mm [width of one of the 35 teeth] and $g = 1$ mm), we obtain $C' = 35.4$ pF/m.

3.2 Force caused by a current element

The current in a metallic wire consists of electrons moving with a drift velocity \mathbf{u} while metal ions, which compensate the negative charge of the electrons towards the outside of the wire, are at rest. The force exerted by a short segment of a wire of length ds at the origin of the coordinate system onto a test charge q is therefore equal

to the sum of the Weber forces of all resting metal ions and all moving electrons in the wire.

We will now calculate this force using the equations derived above. First, the formula of the Weber force (7) must be converted into a more practicable form. Let $\mathbf{v} := \dot{\mathbf{r}}$ be the first time derivative of the distance vector (5) and $\ddot{\mathbf{r}} := \mathbf{a} = \dot{\mathbf{v}}$ be the second derivative. This allows us to set up the equations

$$\dot{r} = \frac{d}{dt} \sqrt{\mathbf{r} \cdot \mathbf{r}} = \frac{\mathbf{r} \cdot \mathbf{v}}{r}, \quad (20)$$

and

$$\ddot{r} = \frac{d}{dt} \dot{r} = \frac{v^2}{r} + \frac{\mathbf{r} \cdot \mathbf{a}}{r} - \frac{(\mathbf{r} \cdot \mathbf{v})^2}{r^3}. \quad (21)$$

Substituting these two equations into the Weber force equation (7) for $\mathbf{a} \approx \mathbf{0}$, we obtain the following force formula in vector notation

$$\mathbf{F}(q_s, q_d, \mathbf{r}, \mathbf{v}) = \left(1 + \frac{v^2}{c^2} - \frac{3}{2} \left(\frac{\mathbf{r} \cdot \mathbf{v}}{c}\right)^2\right) \frac{q_s q_d}{4 \pi \epsilon_0} \frac{\mathbf{r}}{r^3}. \quad (22)$$

Assume that there are n electrons moving in the piece of wire of length ds . The total force \mathbf{F}_T of the wire segment onto a test charge q moving with a velocity \mathbf{v} at location \mathbf{r} is therefore equal to

$$\mathbf{F}_T = \mathbf{F}(-ne, q, \mathbf{r}, \mathbf{v} - \mathbf{u}) + \mathbf{F}(ne, q, \mathbf{r}, \mathbf{v}) = \frac{enq}{8c^2\epsilon_0\pi} \frac{\mathbf{r}}{r^3} \left(3 \frac{(\mathbf{ur})^2}{r^2} - 2u^2 + 4\mathbf{u}\mathbf{v} - 6 \frac{(\mathbf{ur})(\mathbf{vr})}{r^2}\right). \quad (23)$$

Because the drift velocities \mathbf{u} in current-carrying metallic conductors are very small, all terms of order $O(u^2)$ can be neglected and, based on the relation $\mu_0 = 1/(c^2 \epsilon_0)$ and $\mathbf{i} := -ne\mathbf{u}/ds$, we can obtain the approximation

$$\mathbf{F}_T(\mathbf{r}, \mathbf{i}, \mathbf{v}) \approx \frac{q\mu_0 ds}{4\pi} \frac{\mathbf{r}}{r^3} \left(3 \frac{(\mathbf{ir})(\mathbf{vr})}{r^2} - 2\mathbf{i}\mathbf{v}\right). \quad (24)$$

This approximation corresponds to Ampère's original force law (2) from 1822 [3], but not to the Biot-Savart law in combination with the Lorentz force [1].

3.3 Induced voltage in the tube

The formula (24) derived above can now be used to calculate the force that the total current (18) in the two strip lines of Fig. 1 produces on the test charge q in the tube next to the capacitor.

For simplicity, we assume that the strip lines are sufficiently thin that the current can be considered to be a line current. In this case, the force \mathbf{F}_u of the upper microstrip on a charge q at location \mathbf{r} with velocity $\mathbf{v} = v\mathbf{e}_y$ is

$$\mathbf{F}_u = \frac{1}{ds} \int_0^l \mathbf{F}_T(\mathbf{r} - x\mathbf{e}_x, i(x)\mathbf{e}_x, v\mathbf{e}_y) dx. \quad (25)$$

Because the test charges are only located inside the tube, $\mathbf{r} = l\mathbf{e}_x + y\mathbf{e}_y$, with y being the only variable parameter.

The force \mathbf{F}_l of the lower microstrip can be calculated analogously to the force of the upper microstrip, giving

$$\mathbf{F}_l = \frac{1}{ds} \int_0^l \mathbf{F}_T(\mathbf{r} - (x \mathbf{e}_x - g \mathbf{e}_z), -i(x) \mathbf{e}_x, v \mathbf{e}_y) dx. \quad (26)$$

It should be noted that the lower microstrip is not only shifted downward by g , but that the current also flows in the opposite direction.

The total force $\mathbf{F} = \mathbf{F}_u + \mathbf{F}_l$ onto the test charge is the sum of the forces of the upper and lower strip lines. Inserting the current (18) and solving the resulting integrals gives the y -component of the total force:

$$\mathbf{F} \mathbf{e}_y = \frac{1}{4\pi} C' l^3 \mu_0 q U_0 v \omega \alpha(y) e^{i(\omega t + \frac{\pi}{2})}. \quad (27)$$

The auxiliary function $\alpha(y)$ was introduced for readability and is defined as

$$\alpha(y) := \frac{1}{(l^2 + y^2)^{3/2}} - \frac{y^2}{(g^2 + y^2)(g^2 + l^2 + y^2)^{3/2}}. \quad (28)$$

If a charge q is guided along the tube with speed v , work is performed on this charge. Electric voltage U is defined as work per charge and can therefore be calculated by solving the integral

$$U = \frac{1}{q} \int_{-\infty}^{+\infty} \mathbf{F} \mathbf{e}_y dy. \quad (29)$$

The choice of the integration limits can be justified by the fact that work is performed only in the vicinity of the microstrip, and integration at greater distances makes essentially no contribution.

Substituting Equation (27) follows

$$U = \frac{1}{4\pi} C' l^3 \mu_0 U_0 v \omega e^{i(\omega t + \frac{\pi}{2})} \int_{-\infty}^{+\infty} \alpha(y) dy. \quad (30)$$

The calculation of the resulting integral is straightforward and gives

$$\int_{-\infty}^{+\infty} \alpha(y) dy = \frac{2g}{l^3} \arccos\left(\frac{g}{\sqrt{g^2 + l^2}}\right) \approx \frac{g\pi}{l^3}, \quad (31)$$

with the approximation being valid when g is significantly smaller than l , as was the case in our experiment.

If we now substitute this into (30) and compute the absolute value, we obtain the amplitude of the induced voltage

$$\hat{U} = \frac{1}{4} C' g \mu_0 U_0 v \omega. \quad (32)$$

This equation suggests that, if Ampère's force law is valid in its original form, there must also be a small AC voltage

of amplitude \hat{U} that is induced by the capacitor and depends linearly on both the speed v of the electrons and the angular frequency $\omega = 2\pi f$ of the transmitter. This AC voltage operates in addition to the high DC voltage that accelerates the electrons in the tube. However, if the Lorentz force (1) is valid, this AC voltage must not exist due to the product $\mathbf{v} \times \mathbf{B}$.

In total, the capacitor had 35 teeth. Taking this into account and substituting the other experimental parameters: $C' = 35.4$ pF/m, $g = 1$ mm, $U_0 = 2.5$ V, $v \approx 0.0076c \approx 2280000$ m/s into (32), we find that the tube acts like an additional voltage source with an amplitude of approximately 13.9 pV/Hz. This corresponds to a voltage of 0.28 mV at a frequency of 20 MHz and 0.83 mV at 60 MHz.

Given the uncertainties and resulting approximations for the properties of the CCFL tube used in this experiment, these calculated voltages agree surprisingly well with the measured results from the experiment. The function estimated from the measured data was $\hat{U}(f) \approx 11.1$ pV/Hz $\cdot f$, which is close to the theoretically estimated value and represents a relative error of only 0.2. This error is further reduced if the length of the tube and the lateral displacements of the microstrips relative to the tube are taken into account.

3.4 Objections

The experiment performed in this article does not yet provide a final proof that the postulated force actually exists. The results instead should be understood as an indication that such a force could exist, and that further experiments are worthy and necessary. A number of possible reasons may explain the experimental results without Weber electrodynamics, but none of them are plausible or convincing.

A potential explanation for the results of this experiment is that the electric or magnetic field would force the charge carriers in the tube to follow a slightly curved path. This would increase the distance that the charge carriers travel in the tube and, thus, the influence of the resistance. However, this can be ruled out as an explanation because path lengthening occurs both when charging and discharging the transmit capacitor. Consequently, this effect would create a signal with a frequency twice as high and would have no influence on the amplitude of the measured signal. Incidentally, harmonics of this type were not observed during the measurement.

Another potential objection is that the gas is partially ionized when current is flowing in the tube but is not ionized when the current is turned off. The permittivity of the medium in the tube would be expected to be different in both cases, which would affect the sensitivity of the antenna to parasitic electric fields longitudinal to the tube. However, a good conducting medium (eg plasma) usually has a lower permittivity than a gas. For this reason, antenna sensitivity would be expected to be lower when current flows, but in this experiment, the measured

voltages are increased. At the same time, when the CCFL is ignited, the conductivity changes from almost zero to a high value. Differences in the potential inside the tube due to external fields should therefore be compensated by the current. The increase in conductivity should therefore not lead to a rise but instead to a drop in the measured voltage, as was confirmed when a copper wire was soldered in place of the tube. In this case, the sensitivity of the antenna was reduced, except for certain resonance frequencies.

Another objection is that when the polarity of the high voltage is reversed, the reversal of the direction of motion of the electrons in the tube should cause the measured voltage to drop rather than rise. This effect does not occur, because the effect studied herein is caused by the current in the capacitor. Thus, the effect is synchronous with the current. However, the voltage already measured with the high voltage switched off is caused by parasitic electric fields in the longitudinal direction of the tube. These electric fields are synchronous with the voltage in the capacitor. As can be seen from (15) and (16), the current and the voltage are 90° out of phase. Reversing the direction of the electron flow in the tube would cause a phase shift of the effect of the current by 180° . However, the phase shift of both effects with respect to each other does not change, because after the polarity reversal, the phase shift is still 90° . Therefore, no change in the amplitude of the voltage is expected by reversing the polarity of the high voltage.

Moreover, the possibility that the measured signal was injected via the high-voltage source can be excluded. When the cable between the signal generator and antenna (connection (C) in Fig. 2) was disconnected without the signal generator being switched off, no signal was detectable in the noise for frequencies below approx 50 MHz. Above this frequency a very small amplitude was detectable, even with the signal cable disconnected (approximately $15 \mu\text{V}$ at 50 MHz increasing to approximately $100 \mu\text{V}$ at 60 MHz). This finding also appears to be consistent with the results shown in Fig. 5 and Fig. 6, which indicate some sensitivity of the experimental setup in this frequency range.

4 Summary and conclusion

There are two key conclusions from this article.

The first conclusion, which is independent of the experiment described here, is that the original form of Ampère's force law is not fully compatible with the Biot-Savart law and modern electrodynamics because modern electrodynamics, based on the Lorentz electromagnetic force, cannot describe a force component that is both proportional to the speed of the test charge and parallel to the direction of motion [1]. However, it has been mathematically shown that Ampère's original force law does contain such force components. This means that any claim that Ampère's force law and Lorentz force would

be compatible must be clearly rejected for purely formal reasons.

The second conclusion from this article derives from the measured results of the experiment described here, because the results agree remarkably well with the predictions of Weber electrodynamics and Ampère's original force law. However, alternative explanations for these results cannot be completely ruled out. To validate the conclusions presented here, this experiment should be repeated with a type of tube that allows the speed of the electrons to be adjusted. Another option would be to use a superconductor instead of a tube, as the speed of the charge carriers can be varied in superconductors as well.

Because the Maxwell equations and Lorentz force currently represent the foundation of modern physics, it would be enormously important to test in future experiments if Weber electrodynamics is superior in the near field – and there was recently another indication that this could be the case [25]. It should then be a point of intensive research to determine the extent to which statements that are directly or indirectly derived from the Maxwell equations and Lorentz force remain valid. It would also be important to find new field equations that are valid for both the near and far fields. For these reasons, it is important to further investigate this subject experimentally.

Acknowledgements

The author expresses his sincere thanks to Najib Aouni, who brought to his attention that the induction effect studied in this paper could exist.

REFERENCES

- [1] P. Graneau, "Ampere and Lorentz forces", *Physics Letters*, vol. 107 A, no. 5, pp. 235–237, 1985.
- [2] P. Graneau, "Electromagnetic jet-propulsion in the direction of current flow", *Nature*, vol. 295, no. 5847, pp. 311–312, 1982.
- [3] A. K. T. Assis and J. P. M. C. Chaib, "Ampère's electrodynamics: Analysis of the meaning and evolution of Ampère's force between current elements, together with a complete translation of his masterpiece", *Theory of electrodynamic phenomena, uniquely deduced from experience*, C. Roy Keys Inc., 2015.
- [4] A. K. T. Assis and M. A. Bueno, "Equivalence between Ampere and Grassmann's forces", *IEEE Transactions On Magnetism*, vol. 32, no. 2, pp. 431–436, 1996.
- [5] J. P. M. C. Chaib and F. M. S. Lima, "Resuming Ampère's experimental investigation of the validity of Newton's third law in electrodynamics", *Annales de la Fondation Louis de Broglie*, vol. 45, no. 1, pp. 19–51, 2020.
- [6] J. P. Wesley, "Weber electrodynamics, Part I. General theory, steady current effects", *Foundations of Physics Letters*, vol. 3, no. 5, pp. 443–469, 1990.
- [7] M. Tajmar and M. Weikert, "Evaluation of the influence of a field-less electrostatic potential on electron beam deflection as predicted by Weber electrodynamics", *Progress In Electromagnetics Research M*, vol. 105, pp. 1–8, 2021.
- [8] A. K. T. Assis and M. Tajmat, "Rotation of a superconductor due to electromagnetic induction using Weber's electrodynamics", *Annales de la Fondation Louis de Broglie*, vol. 44, pp. 111–123, 2019.

- [9] C. Baumgärtel and M. Tajmar, “The Planck constant and the origin of mass due to a higher order Casimir effect”, *Journal of Advanced Physics*, vol. 7, no. 1, pp. 135–140, 2018.
- [10] R. T. Smith and S. Maher, “Investigating electron beam deflections by a long straight wire carrying a constant current using direct action, emission-based and field theory approaches of electrodynamics”, *Progress In Electromagnetics Research B*, vol. 75, pp. 79–89, 2017.
- [11] A. K. T. Assis and M. Tajmar, “Superconductivity with Weber’s electrodynamics: the London moment and the Meissner effect”, *Annales de la Fondation Louis de Broglie*, vol. 42, no. 2, pp. 307–350, 2017.
- [12] R. T. Smith, F. P. M. Jjunju, and S. Maher, “Evaluation of electron beam deflections across a solenoid using Weber-Ritz and Maxwell-Lorentz electrodynamics”, *Progress In Electromagnetics Research*, vol. 151, pp. 83–93, 2015.
- [13] H. Torres-Silva, J. López-Bonilla, R. López-Vázquez, and J. Rivera-Rebolledo, “Weber’s electrodynamics for the hydrogen atom”, *Indonesian Journal of Applied Physics*, vol. 5, no. 1, pp. 39–46, 2015.
- [14] R. T. Smith, S. Taylor, and S. Maher, “Modelling electromagnetic induction via accelerated electron motion”, *Canadian Journal of Physics*, vol. 93, no. 7, pp. 802–806, 2015.
- [15] M. Tajmar and A. K. T. Assis, “Gravitational induction with Weber’s force”, *Canadian Journal of Physics*, vol. 93, no. 12, pp. 1571–1573, 2015.
- [16] R. T. Smith, F. P. M. Jjunju, I. S. Young, S. Taylor, and S. Maher, “A physical model for low-frequency electromagnetic induction in the near field based on direct interaction between transmitter and receiver electrons”, *Proceedings of the Royal Society A: Mathematical, Physical and Engineering Sciences*, vol. 472:0338, 2016.
- [17] H. Härtel, “Electromagnetic induction from a new perspective” *European J. of Physics Education*, vol. 9, no. 2, pp. 29–36, 2018.
- [18] A. K. T. Assis and H. T. Silva, “Comparison between Weber’s electrodynamics and classical electrodynamics”, *Pramana*, vol. 55, pp. 393–404, 2000/2018.
- [19] T. E. Phipps, “Toward modernization of Weber’s force law”, *Physics Essays*, vol. 3, no. 4, pp. 414–420, 1990.
- [20] J. M. Montes, “On limiting velocity with Weber-like potentials”, *Canadian Journal of Physics*, vol. 95, no. 8, pp. 770–776, 2017.
- [21] A. K. T. Assis, “Deriving Ampere’s law from Weber’s law”, *Hadronic Journal*, vol. 13, pp. 441–451, 1990.
- [22] L. Page and N. I. Adams Jr, “Action and reaction between moving charges”, *American Journal of Physics*, vol. 13, no. 3, pp. 141–147, 1945.
- [23] J. H. Kahl, “Cold cathode fluorescent lamps (CCFL’s): A history and overview”, *JKL Components Corporation, Tech. Rep*, 1997.
- [24] S. Kühn, “General analytic solution of the telegrapher’ equations and the resulting consequences for electrically short transmission lines”, *Journal of Electromagnetic Analysis and Applications*, vol. 12, pp. 71–87, 2020.
- [25] C. Baumgärtel, R. T. Smith, and S. Maher, “Accurately predicting electron beam deflections in fringing fields of a solenoid”, *Scientific Reports*, vol. 10, no. 1, p. 10903, 2020.

Received 25 September 2021

Steffen Kühn is a developer of electronic devices, such as measuring instruments, data loggers, consumer electronics and medical technology for various clients for more than 20 years, mainly he develops hardware, operating systems, mathematical software or implements customizations in the Linux kernel. From 2004 to 2009 he was a research assistant at the Technical University of Berlin, Chair of Electronic Measurement and Diagnostic Technology. In 2010, received the PhD in electrical engineering. His research was focused on the analysis of sensor data with AI. He is co-founder and CTO of the AURI-NOVO GmbH, near Berlin, which develops network-less and secure speech recognition electronics. He also research open questions in the foundations of physics.